



Catalytic Reduction of N₂ to Borylamine at a Molybdenum Complex

Soukaina Bennaamane, Maria F Espada, Andrea Mulas, Théo Personeni, Nathalie Saffon-Merceron, Marie Fustier-Boutignon, Christophe Bucher, Nicolas Mézailles

► To cite this version:

Soukaina Bennaamane, Maria F Espada, Andrea Mulas, Théo Personeni, Nathalie Saffon-Merceron, et al.. Catalytic Reduction of N₂ to Borylamine at a Molybdenum Complex. *Angewandte Chemie International Edition*, 2021, 60 (37), pp.20210-20214. <10.1002/anie.202106025>. <hal-03758782>

HAL Id: hal-03758782

<https://hal.science/hal-03758782v1>

Submitted on 23 Aug 2022

HAL is a multi-disciplinary open access archive for the deposit and dissemination of scientific research documents, whether they are published or not. The documents may come from teaching and research institutions in France or abroad, or from public or private research centers.

L'archive ouverte pluridisciplinaire **HAL**, est destinée au dépôt et à la diffusion de documents scientifiques de niveau recherche, publiés ou non, émanant des établissements d'enseignement et de recherche français ou étrangers, des laboratoires publics ou privés.



HAL Authorization

Catalytic Reduction of N₂ to Borylamine at a Molybdenum Complex

Soukaina Bennaamane,^[a] Maria F. Espada,^[a] Andrea Mulas,^[c] Théo Personeni,^[c] Nathalie Saffon-Merceron,^[b] Marie Fustier-Boutignon,^[a] Christophe Bucher,^{[c]*} Nicolas Mézailles^{[a]*}

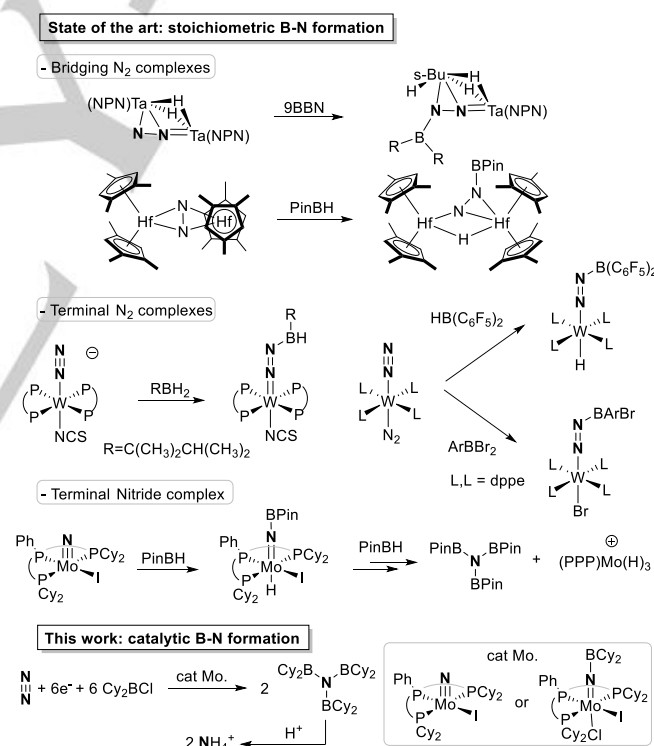
Dedication: In memory of Pascal Le Floch.

Abstract: Catalytic formation of borylamines from atmospheric N₂ is achieved for the first time using a series of homogenous (triphosphine)Mo complexes. Stepwise functionalization of the (triphosphine)Mo-nitrido complex with chloroborane led the synthesis of the imido complex. Electrochemical characterization of the (PPP)Mo-nitrido and (PPP)Mo-borylimido complexes showed that the latter is much more easily reduced.

N₂ fixation using homogeneous metal complexes has been studied actively over the past decades.^[1-12] These intense efforts have culminated in the discovery of only two catalytic processes, N₂-to-NH₃,^[13-19] and N₂-to-NTMS₃,^[20-26] using carefully designed metal complexes.^[27-32] In these processes, N₂ is coordinated to the metal center and subsequently functionalized using external sources of electrons and electrophiles (H⁺ and R₃SiCl, respectively). Mechanistically speaking, NH bonds can be obtained via stepwise and/or coupled H⁺/e⁻ transfers,^[13,33] while it is proposed that the NSi bond formation occurs via Si radicals.^[20,21] Most importantly, Nishibayashi recently showed that the activation path involved with a given PNPMo fragment depends on the sources of protons and electrons used.^[19,34] Functionalization of N₂ with main group elements was studied early on by Hidai and coworkers. These pioneering works carried out with W⁽⁰⁾ most notably revealed that BH bonds react with metal coordinated N₂ to yield diazenido W(N=NBHR) complexes.^[35] Simonneau further explored this reactivity using strongly electrophilic derivative (C₆F₅)₂BH.^[36,37] In 2020, Braunschweig reported the 1,3 addition of a B-Br bond across a W-NN moiety.^[38] Using early transition metals, Fryzuk achieved the 1,2 B-H addition on N₂ at a bimetallic Ta complex,^[39] while Chirik observed the formation of a N-B bond and bridging hydride starting from a side on MN₂M (M= Zr, Hf) complex.^[40] We have also made a significant contribution to this field upon showing that a Mo-nitrido complex, obtained by direct splitting of N₂, reacts towards mild electrophiles such as PinBH,^[41,42] to afford borylamines via stepwise functionalization of the N center.

However, so far none of the above mentioned N-B bond forming reactions have led to the development of catalytic processes.

We report here the first catalytic reduction of N₂ into borylamines using chloroboranes as electrophilic substrate (Scheme 1). Mechanistic investigations reveal that the catalytic process proceeds through a fast 1,2-addition of B-Cl across the Mo≡N bond to form a stable borylimido intermediate. Electrochemical studies carried out on these compounds also demonstrate that the addition of B-Cl leads to a significant positive shift of the metal-centered reduction potential, i.e. that the Mo^(IV) center is easier to reduce in the borylimido intermediate than in the starting nitrido.



Scheme 1. Approaches to N₂ functionalization by boron derivatives: stoichiometric and catalytic N-B bond formation.

In 2015, we reported the stepwise functionalization of [(P^{Ph}P₂Cy₂)Mo⁽⁰⁾(N₂)₂(μ-N₂)] by R₃SiCl/electrons, and characterization of key intermediates, including the hydrazido Mo^(IV)=N-N(SiR₃)₂, nitrido Mo^(IV)≡N and imido Mo^(IV)=NSiR₃ complexes.^[22] All complexes proved equally efficient for the catalytic production of N(SiMe₃)₃. The nitrido complex **2** [(P^{Ph}P₂Cy₂)Mo(N)(I)], which was found to be highly reactive towards silane (Si-H) and borane (B-H) derivatives,^[42,43]

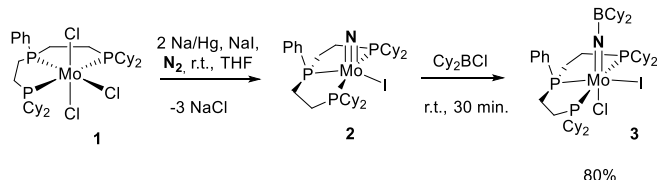
[a] Dr. S. Bennaamane, Dr. M.F.Espada, Dr. M. Fustier-Boutignon, Dr. N. Mézailles

Laboratoire Hétérochimie Fondamentale et Appliquée
Université Paul Sabatier, CNRS
118 Route de Narbonne, 31062 Toulouse (France)
E-mail: mezailles@chimie.ups-tlse.fr

[b] Dr. N. Saffon-Merceron
Institut de Chimie de Toulouse ICT-FR2599
Université Paul Sabatier, CNRS
31062 Toulouse Cedex (France)

[c] Dr. A. Mulas, T. Personeni, Dr. C. Bucher
Univ Lyon, ENS Lyon, CNRS, Université Lyon 1, Laboratoire de Chimie,
UMR 5182, 46 allée d'Italie, 69364 Lyon (France)
E-mail: christophe.bucher@ens-lyon.fr

appeared as a highly relevant starting material for the present study. The reactivity of **2** towards Cy_2BCl was first revealed by marked color changes, observed upon simple mixing of stoichiometric amounts of both compounds in THF at room temperature (λ_{max} going from 415 to 394 nm, Fig. S14 and S15). Formation of the imido complex **3** was further demonstrated by ^{31}P NMR, through the downfield shift of both singlets up to 102.3 ($\Delta\delta = +20$ ppm) and 61.9 ppm ($\Delta\delta = +6$ ppm).



Scheme 2. N_2 splitting and 1,2 B-Cl addition across MoN.

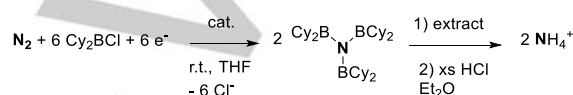
Complex **3** was isolated as a greenish solid in a very good 80% yield and characterized by multinuclear NMR spectroscopy. No signal was observed in the $^{11}\text{B}\{^1\text{H}\}$ spectrum, as often encountered for tricoordinated B centers, especially when they are bonded to a quadrupolar center such as N.^[38] X-ray diffraction analysis of crystals obtained by diffusion of pentane into a THF solution of the complex provided definitive proof of the proposed structure (see ESI).^[44] The Mo1–N1 bond distance of 1.746(2) Å is much longer than in the starting Mo^{IV} -nitrido complex **2** (1.656(2) Å), indicative of a decrease in bond order expected upon functionalization. It is also found slightly shorter than the bond measured in the related trans hydrido-borylimido complex obtained from PinBH (1.784(3) Å), most likely as a result of the weaker trans effect of Cl compared to H.

Reactivity studies involved assessing the catalytic activities of the four isolated Mo complexes, i.e. $[(\text{P}^{\text{Ph}}\text{P}_2^{\text{Cy}})\text{MoCl}_3]$ **1**, $[(\text{P}^{\text{Ph}}\text{P}_2^{\text{Cy}})\text{Mo}(\text{N})\text{I}]$ **2**, $[(\text{P}^{\text{Ph}}\text{P}_2^{\text{Cy}})\text{MoCl}(\text{NBCy}_2)]$ **3**, and $[(\text{P}^{\text{Ph}}\text{P}_2^{\text{Cy}})\text{Mo}(\text{N}_2)_2(\mu\text{-N}_2)]$ **4**,^[20] for the reduction of N_2 by chloroborane/electrons.

First optimizations studies were carried out with complex $[(\text{P}^{\text{Ph}}\text{P}_2^{\text{Cy}})\text{MoCl}_3]$ **1**. Quantification of the N containing products was achieved with a well proven procedure (see ESI). The first positive result was obtained with Na/Hg (200 eq.) used as reducing agent (entry 1), which provided 3.3 equivalents of NH_4^+ . Changing to K (200 eq.) doubled the TON. Interestingly, decreasing the amount of K/ Cy_2BCl led to a drastic increase in the yields (entries 4 vs 3 vs 2), reaching 85%, coming along with a slight increase of the TON (entry 4, TON = 9.0). Further investigations carried out with the parent nitrido and borylimido complexes **2** and **3** gave similar results, with yield reaching up to 90.6 % (entries 4-6).^[45] On the other hand, the $[(\text{P}^{\text{Ph}}\text{P}_2^{\text{Cy}})\text{Mo}(\text{N}_2)_2(\mu\text{-N}_2)]$ Mo^{IV} complex **4** turned out to be slightly less efficient (entry 7 vs 5).

We studied next the influence of different parameters on the catalytic activity of complex **2**. No formation of NH_4^+ was seen at -60°C and -40°C (entries 8 and 9), despite increased solubility of N_2 at low temperature. A TON of 15 was nevertheless obtained upon slowly raising the temperature between -60°C and 20°C (entry 10). On the other hand, performing the reaction above room temperature was found to

decrease the yield very significantly, becoming nearly null at 60°C likely because of the decreased solubility of N_2 near the boiling point of the solvent (entries 11 and 12 vs 5). Efforts were then paid to increase the overall TON. An increase of more than 50% was obtained by doubling the amount of K/ Cy_2BCl (entries 5 and 13, TON 14.6 vs 9.6). Further addition of K/ Cy_2BCl only led to slight increase of the TON (up to 20.0, entries 15 and 16), however at the expense of yield, which dropped drastically down to 15%. Finally, entry 14 shows that the catalyst is decomposed within 6 h, as reloading did not increase the overall TON. Overall, the best TON for this very first example of catalytic production of N-B bond remains limited, but the yield can be very high (ca 90%). Clearly, this demonstrates that side reactions leading to catalyst decomposition become competitive at lower catalyst loading, i.e. when larger amounts of reducing agent and chloroborane are used. Further optimization will be required to improve this process both in terms of TON and yield.



Scheme 3. Catalytic process.

Entry	Cat.	temp	Red	Equiv e/BCl	TON	TON max	Yield d. %
1	1	r.t.	Na/ Hg	200	3.3	66.6	4.7
2	1	r.t.	K	200	6.2	66.6	9.3
3	1	r.t.	K	100	6.6	33.3	18.2
4	1	r.t.	K	32	9.0±1.0	10.6	84.9
5	2	r.t.	K	32	9.6±2.0	10.6	90.6
6	3	r.t.	K	32	8.3±2.0	10.6	78.3
7	4	r.t.	K	32	6.6±1.0	10.6	62.3
8	2	-60	K	100	0	33.3	0
9	2	-40	K	100	0	33.3	0
10	2	-60 - r.t.	K	100	15.0	33.3	45.5
11	2	35	K	32	4.5	10.6	42.5
12	2	60	K	32	0.5	10.6	1.6
13	2	r.t.	K	66	14.6±1.0	22	66.4
14	2	r.t.	K	66+66	14.0	22+22	30.9
15	2	r.t.	K	120	20.0	40	50.0
16	2	r.t.	K	400	20.0	133.3	15.0

Table 1: Standard conditions unless otherwise mentioned: 0.005 mmol catalyst, stoichiometric amount of reducing agent and Cy_2BCl , THF (6 mL), r. t. (ca 20°C) 12 h, fast stirring under N_2 . The TON is an average of three to five experiments for entries 4-7 and 12 (standard variation is given). "TON" is defined as the amount of NH_4^+ formed per complex. TONmax is calculated considering the formation of $\text{N}(\text{BCy}_2)_3$, yield = $\text{TON}/\text{TONmax} \times 100$.

Labelling experiments were conducted to identify the N containing product(s) synthesized through this catalytic process. Formation of NH_4^+ can potentially originate from the hydrolysis of $\text{N}(\text{BCy}_2)_3$, $\text{N}(\text{BCy}_2)_2^-$ or $\text{NH}(\text{BCy}_2)_2$ or of a mixture of these species.^[20] A mixture of $^{15}\text{N}_2$ and $^{14}\text{N}_2$ was thus used in an

attempt to identify the precursor of NH_4^+ (see ESI for the detailed experiment). The crude mixture was analyzed by $^{15}\text{N}\{^1\text{H}\}$ and $^{15}\text{N}\text{-}^1\text{H}$ HSQC NMR experiments, as well as by ^1H NMR before and after hydrolysis. The ^1H NMR spectrum recorded after hydrolysis with excess HCl revealed the formation of both $^{14}\text{NH}_4^+$ and $^{15}\text{NH}_4^+$ (Fig. S7), with an overall TON of 10.6. As expected, the ^1H spectrum recorded before hydrolysis displays very intense multiplets attributed to the cyclohexyl substituents (Fig. S3). The $^{15}\text{N}\text{-}^1\text{H}$ HSQC is a very sensitive technique to detect the presence of N-H bonds. In the spectrum recorded before workup, the formation of $(\text{Cy}_2\text{B})_2\text{NH}$ was evidenced by a cross correlation between two signals resonating at 123 ppm (^{15}N) and 6.2 ppm (^1H) (Fig. S4). Integration of the signal at 6.2 ppm vs that of the cyclohexyl substituents in the ^1H spectrum however clearly showed that $(\text{Cy}_2\text{B})_2\text{NH}$ was only formed as traces (Fig. S3). Accordingly, despite ^{15}N enrichment, the 1D ^{15}N spectrum shows a very weak signal at 123 ppm (Fig. S6), and no signal for the other possible N derivatives formed during the catalytic process ($\text{N}(\text{BCy}_2)_3$ or $\text{N}(\text{BCy}_2)_2$). Most importantly however, protonation of this crude mixture with lutidinium OTf did not result in the significant formation of $\text{N}(\text{BCy}_2)_3$, thereby ruling out the formation of $\text{N}(\text{BCy}_2)_2$. Finally, the mass spectrum (ESI in negative mode, Fig. S5) recorded for a crude mixture after completion of the catalytic experiments clearly revealed the formation of $\text{N}(\text{BCy}_2)_3$. In conclusion, the ^{15}N labelling experiment together with NMR and MS characterizations support the catalytic formation of $(\text{Cy}_2\text{B})_3\text{N}$ from N_2 via the catalytic process. The absence of a specific signal in the ^{15}N NMR spectrum for this species most likely result from massive broadening due to the coupling of the N center with three neighboring B nuclei (^{11}B decoupling cannot be done for the recording of the 1D ^{15}N NMR spectrum).

Further insights into the N_2 reduction mechanism was provided by electrochemical investigations carried out on the nitrido complex **2** [$(\text{P}^{\text{Ph}}\text{P}_2^{\text{Cy}})\text{Mo}(\text{N})(\text{I})$] in the absence and in the presence of Cy_2BCl (exp. details, see ESI). The CV curves of complex **2** recorded in the anodic and cathodic potential domains at a vitreous carbon working electrode are depicted as bold lines in figure 1A and 1B, respectively. The latter display one reversible oxidation at $(E_{1/2})_{\text{a}} = -0.7$ V (vs Ag^+/Ag) attributed to the one-electron oxidation of **2** yielding $[(\text{P}^{\text{Ph}}\text{P}_2^{\text{Cy}})\text{Mo}^{\text{V}}(\text{N})(\text{I})]^+$, whose stability at the CV time scale is revealed by the reversibility of the wave. On the cathodic side, the large accessible potential window associated to the THF/TBATFSI electrolyte enables to observe one fully irreversible reduction wave at $E_{\text{peak}} \sim -3$ V attributed to the in-situ formation of a reactive Mo^{III} complex. The fate of this intermediate still remains to be established but one path currently considered to account for the experimental data involves the ejection of a coordinated iodide ligand to stabilize the electron-rich Mo^{III} center.

As can be seen in Figure 1, addition of Cy_2BCl led to drastic changes in the CV curves consistent with the formation of a single well-defined product in solution. On the anodic side, repeated addition of aliquots of Cy_2BCl (curves (b)–(d) Figure 2B) led to the progressive disappearance of the initial signal at the expense of a new reversible wave, emerging at a more positive potential value $(E_{1/2})_{\text{d}} = -0.35$ V, attributed to the electron oxidation of the *in-situ* generated complex **3**

$[(\text{P}^{\text{Ph}}\text{P}_2^{\text{Cy}})\text{Mo}^{\text{IV}}\text{Cl}(\text{NBCy}_2)]$ (identical to the CV obtained from an authentic sample of complex **3**, Fig. S12). This large positive potential shift, of about 350 mV, observed between **2** and **3**, is consistent with the addition of an electron-withdrawing chloride ligand at the Mo^{IV} center and of a boryl moiety at N, thus making it much harder to oxidize. Here again, the reversible character of the wave reveals the stability of $[(\text{P}^{\text{Ph}}\text{P}_2^{\text{Cy}})\text{Mo}^{\text{IV}}\text{Cl}(\text{NBCy}_2)]$ and of $[(\text{P}^{\text{Ph}}\text{P}_2^{\text{Cy}})\text{Mo}^{\text{V}}\text{Cl}(\text{NBCy}_2)]^+$ at the CV time scale.

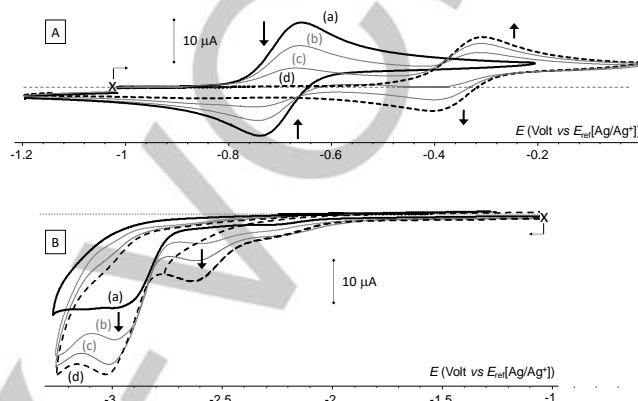


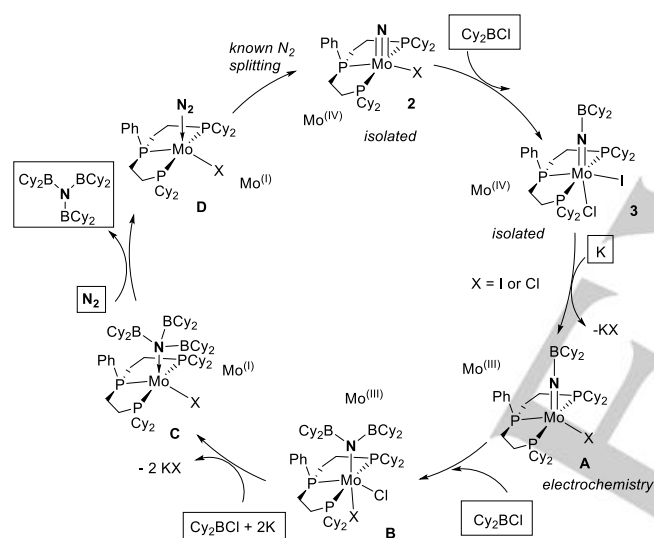
Figure 1. Cyclic Voltammetry of Complex **2** (bold line) and evolution upon addition of 0.25, 0.75 and 1.0 equivalent of Cy_2BCl (traces (b), (c) and (d) respectively). (100 mV/s, vitreous carb \varnothing 3 mm, THF + TBATFSI 0.2 M).

A similar 350 mV positive shift of the reduction wave was monitored on the cathodic side upon addition of Cy_2BCl (Figure 2B), with a novel irreversible wave developing at ca $E_{\text{peak}} \sim -2.65$ V, attributed to the one electron reduction of the Mo center in $[(\text{P}^{\text{Ph}}\text{P}_2^{\text{Cy}})\text{Mo}^{\text{IV}}\text{Cl}(\text{NBCy}_2)]$ complex **3** (Fig. S13), an attribution which is supported by the fact that the HOMO-LUMO gap is kept constant through the conversion **2** \rightarrow **3**. As observed with **2** and in full agreement with the mechanism proposed in Scheme 3, the irreversible character of this new reduction wave, observed at all investigated scan rates (0.1–2 V/s), put forward the reactivity of the electrochemically reduced Mo^{III} complex.

Taken together, these electrochemical data support the conclusion that **2** readily reacts with Cy_2BCl to yield the borylimido Mo^{IV} complex **3** which is both harder to oxidize and easier to reduce as the result of the ligation of NBCy_2 and Cl ligands on the Mo center. Attribution of the two accessible redox processes observed in **2** and **3** to the same metal-centered electron transfers is supported by limited changes in the HOMO-LUMO gaps. Most importantly, the great reactivity of the reduced forms of **2** and **3** are revealed by the irreversible character of the $\text{Mo}^{\text{IV}}/\text{Mo}^{\text{III}}$ reduction waves.

Overall, these preliminary results provide clear insights into important steps of the catalytic process involved in solution. Thus, from the nitrido complex **2**, fast addition of Cy_2BCl results in the formation of the borylimido Mo^{IV} complex **3**, followed by a one-electron reduction of the Mo center leading to the borylimido Mo^{III} complex **A**. This key in situ-generated reactive intermediate features an unsaturated, albeit electron-rich, metal center which reacts with Cy_2BCl to afford the bis-borylamido

Mo^(III) complex **B**. In the mechanism proposed in Scheme 3, this complex is subjected to another two electron reduction and to a reaction with a third equivalent of Cy₂BCl to give the trisborylamine complex Mo⁽⁰⁾ **C**. The final step allowing closing the catalytic cycle is a ligand exchange between the amine and N₂ yielding the Mo⁽⁰⁾(N₂) complex **D** which is known to split N₂ with regeneration of the initial nitrido complex **2**. In depth mechanistic investigations are currently underway to isolate other intermediates of the proposed mechanism. To probe the relevance of an alternative mechanism involving a Mo⁽⁰⁾ dinitrogen intermediate, we reacted complex **4** with two equiv. of Cy₂BCl. The fact that no reaction was observed after stirring the mixture for 48h at r.t. shows that complex **4** is converted into a catalytically active complex only in the presence of excess Cy₂BCl and K (catalytic conditions). The Mo⁽⁰⁾ dinitrogen complex **4** would thus act as a pre-catalyst rather than a real intermediate in the catalytic cycle. Nonetheless, at this point, we cannot definitively rule out the intermediacy of Mo⁽⁰⁾ in a competitive catalytic cycle.



Scheme 3. Proposed mechanism for the catalytic reduction of N₂.

In conclusion, we present here a new catalytic process to transform N₂. For the first time, N-B bonds can be prepared directly from N₂ using Cy₂BCl and K as sources of electrophile and electrons, respectively. At high catalyst loading, the process is highly efficient, but when a large excess of reducing agent and chloroborane are present, decomposition pathways become competitive. The electrochemical study corroborates that at high reducing power, the Mo complexes can be reduced simultaneously, providing deactivation pathways. Efforts are currently dedicated to optimize this novel process, in particular using electrochemical approach and more selective reducing agents.

Acknowledgements

Financial support from CNRS and Université de Toulouse is acknowledged. N.M. thanks the IDEX of the Université Fédérale Toulouse Midi-Pyrénées for generous funding, including post-doctoral fellowship for M.F.E.. S.B. is grateful to the ANR (CaDeSMARE) for a Ph.D fellowship. C.B. wishes to thank the "région Auvergne-Rhône-Alpes" for financial support. The NMR service of the ICT is gratefully acknowledged. We thank Solvay for a generous gift of phosphines.

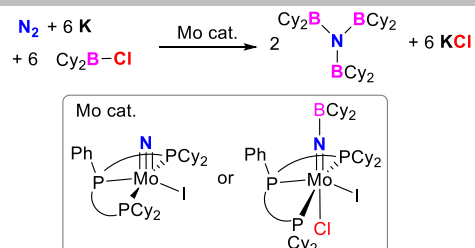
Keywords: N₂ reduction • Molybdenum • boranes • nitride functionalization • tridentate phosphine ligands

- [1] C. E. Laplaza, C. C. Cummins, *Science* **1995**, *268*, 861–863.
- [2] M. D. Fryzuk, J. B. Love, S. J. Rettig, V. G. Young, *Science* **1997**, *275*, 1445–1447.
- [3] J. A. Pool, E. Lobkovsky, P. J. Chirik, *Nature* **2004**, *427*, 527–530.
- [4] M. D. Fryzuk, *Acc. Chem. Res.* **2009**, *42*, 127–133.
- [5] M. M. Rodriguez, E. Bill, W. W. Brennessel, P. L. Holland, *Science* **2011**, *334*, 780–783.
- [6] T. Shima, S. Hu, G. Luo, X. Kang, Y. Luo, Z. Hou, *Science* **2013**, *340*, 1549–1552.
- [7] T. Shima, S. Hu, G. Luo, X. Kang, Y. Luo, Z. Hou, *Science* **2013**, *340*, 1549–1552.
- [8] K. P. Chiang, S. M. Bellows, W. W. Brennessel, P. L. Holland, *Chem. Sci.* **2014**, *5*, 267–274.
- [9] M. J. Bezdek, S. Guo, P. J. Chirik, *Science* **2016**, *354*, 730–733.
- [10] Y. Nishibayashi, Ed., *Transition Metal-Dinitrogen Complexes, Preparation and Reactivity*, Wiley-VCH, Weinheim, **2019**.
- [11] S. F. McWilliams, D. L. J. Broere, C. J. V. Halliday, S. M. Bhutto, B. Q. Mercado, P. L. Holland, *Nature* **2020**, *584*, 221–226.
- [12] J. Song, Q. Liao, X. Hong, L. Jin, N. Mézailles, *Angew. Chem. Int. Ed.* **2021**, DOI 10.1002/anie.202015183.
- [13] D. V. Yandulov, R. R. Schrock, *Science* **2003**, *301*, 76–78.
- [14] K. Arashiba, Y. Miyake, Y. Nishibayashi, *Nature Chem.* **2011**, *3*, 120–125.
- [15] J. S. Anderson, J. Rittle, J. C. Peters, *Nature* **2013**, *501*, 84–87.
- [16] S. Kuriyama, K. Arashiba, K. Nakajima, H. Tanaka, N. Kamaru, K. Yoshizawa, Y. Nishibayashi, *J. Am. Chem. Soc.* **2014**, *136*, 9719–9731.
- [17] K. Arashiba, E. Kinoshita, S. Kuriyama, A. Eizawa, K. Nakajima, H. Tanaka, K. Yoshizawa, Y. Nishibayashi, *J. Am. Chem. Soc.* **2015**, *137*, 5666–5669.
- [18] L. A. Wickramasinghe, T. Ogawa, R. R. Schrock, P. Müller, *J. Am. Chem. Soc.* **2017**, *139*, 9132–9135.
- [19] Y. Ashida, K. Arashiba, K. Nakajima, Y. Nishibayashi, *Nature* **2019**, *568*, 536–540.
- [20] K. Komori, H. Oshita, Y. Mizobe, M. Hidai, *J. Am. Chem. Soc.* **1989**, *111*, 1939–1940.
- [21] H. Tanaka, A. Sasada, T. Kouno, M. Yuki, Y. Miyake, H. Nakanishi, Y. Nishibayashi, K. Yoshizawa, *J. Am. Chem. Soc.* **2011**, *133*, 3498–3506.
- [22] Q. Liao, N. Saffon-Merceron, N. Mézailles, *ACS Catal.* **2015**, *5*, 6902–6906.
- [23] R. B. Siedschlag, V. Bernales, K. D. Vogiatzis, N. Planas, L. J. Clouston, E. Bill, L. Gagliardi, C. C. Lu, *J. Am. Chem. Soc.* **2015**, *137*, 4638–4641.
- [24] D. E. Prokopchuk, E. S. Wiedner, E. D. Walter, C. v. Popescu, N. A. Piro, W. S. Kassel, R. M. Bullock, M. T. Mock, *J. Am. Chem. Soc.* **2017**, *139*, 9291–9301.
- [25] T. Suzuki, K. Fujimoto, Y. Takemoto, Y. Wasada-Tsutsui, T. Ozawa, T. Inomata, M. D. Fryzuk, H. Masuda, *ACS Catal.* **2018**, *8*, 3011–3015.
- [26] A. D. Piascik, R. Li, H. J. Wilkinson, J. C. Green, A. E. Ashley, *J. Am. Chem. Soc.* **2018**, *140*, 10691–10694.
- [27] M. J. Chalkley, M. W. Drover, J. C. Peters, *Chem. Rev.* **2020**, *120*, 5582–5636.
- [28] S. Kim, F. Loose, P. J. Chirik, *Chem. Rev.* **2020**, *120*, 5637–5681.

- [29] Y. Ashida, Y. Nishibayashi, *Chem. Commun.* **2021**, 57, 1176–1189.
- [30] Y. Tanabe, Y. Nishibayashi, *Chem. Soc. Rev.* **2021**, 50, 5201.
- [31] F. Masero, M. A. Perrin, S. Dey, V. Mougél, *Chem. Eur. J.* **2021**, 27, 3892–3928.
- [32] N. Mézailles, in *Reference Module in Chemistry, Molecular Sciences and Chemical Engineering*, Elsevier, **2021**. <https://doi.org/10.1016/B978-0-08-102688-5.00083-0>
- [33] D. v. Yandulov, R. R. Schrock, *Inorg. Chem.* **2005**, 44, 1103–1117.
- [34] K. Arashiba, A. Eizawa, H. Tanaka, K. Nakajima, K. Yoshizawa, Y. Nishibayashi, *Bull. Chem. Soc. Japan* **2017**, 90, 1111–1118.
- [35] H. Ishino, Y. Ishii, M. Hidai, *Chem. Lett.* **1998**, 677–678.
- [36] A. Simonneau, R. Turrel, L. Vendier, M. Etienne, *Angew. Chem. Int. Ed.* **2017**, 56, 12268–12272.
- [37] A. Coffinet, D. Specklin, L. Vendier, M. Etienne, A. Simonneau, *Chem. Eur. J.* **2019**, 25, 1–5.
- [38] A. Rempel, S. K. Møllerup, F. Fantuzzi, A. Herzog, A. Deißberger, R. Bertermann, B. Engels, H. Braunschweig, *Chem. Eur. J.* **2020**, 26, 16019–16027.
- [39] M. D. Fryzuk, B. A. MacKay, S. A. Johnson, B. O. Patrick, *Angew. Chem. Int. Ed.* **2002**, 41, 3709–3712.
- [40] S. P. Semproni, P. J. Chirik, *Eur. J. Inorg. Chem.* **2013**, 3907–3915.
- [41] Q. Liao, A. Cavaillé, N. Saffon-Merceron, N. Mézailles, *Angew. Chem. Int. Ed.* **2016**, 55, 11212–11216.
- [42] M. F. Espada, S. Bennaamane, Q. Liao, N. Saffon-Merceron, S. Massou, E. Clot, N. Nebra, M. Fustier-Boutignon, N. Mézailles, *Angew. Chem. Int. Ed.* **2018**, 57, 12865–12868.
- [43] S. Bennaamane, M. F. Espada, I. Yagoub, N. Saffon-Merceron, N. Nebra, M. Fustier-Boutignon, E. Clot, N. Mézailles, *Eur. J. Inorg. Chem.* **2020**, 1499–1505.
- [44] CCDC-2081288 (3) contains the supplementary crystallographic data for this paper.
- [45] Separation of the inorganic species from the organics after a catalytic test (entry 5) prior to hydrolysis resulted in a lowering of TON by 0.5. It shows that the unknown paramagnetic “Mo” residue resulting from catalysis contains Mo-N bond.

COMMUNICATION

Catalytic formation of N-B bonds from atmospheric N₂, chloroboranes and electrons is achieved with (triphosphine)Mo complexes.



Soukaina Bennaamane, Maria F. Espada, Andrea Mulas, Théo Personeni, Nathalie Saffon-Merceron, Marie Fustier-Boutignon, Christophe Bucher* and Nicolas Mézailles*

Page No. – Page No.

Catalytic Reduction of N₂ to Borylamine at a Mo Complex